

mission of the return beam is  $\geq 60\%$  with respect to the unaberrated beam. In prior TNL experiments with 30-ns Q-switched Nd:glass lasers, the measured fidelity was about 5%.<sup>1</sup>

This work was supported by a contract from ARPA (MDA972-94-3-0020).

1. A. A. Betin, A. V. Kirsanov, *Kvantovaya Elektronika* 21(3), 237-240 (1994) (in Russian).

**CFG** 10:30 am  
Room B2

**WDM Network Technology**

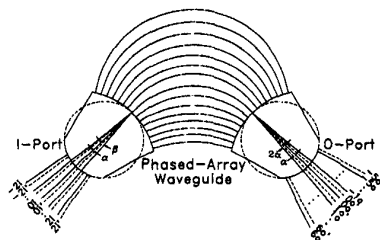
Evan Lee Goldstein, *AT&T Bell Laboratories, Presider*

**CFG1** 10:30 am

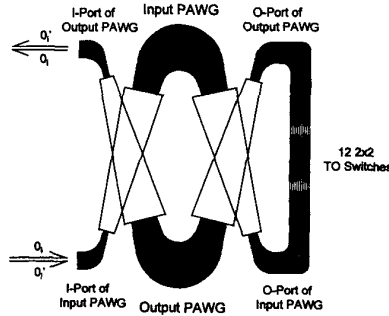
**8-channel wavelength-selective 2 x 2 optical switch using phased-array waveguide grating multi/demultiplexer**

Haifeng Li, Wenhua Lin, Y. J. Chen, D. Stone, *Department of Computer Science and Electrical Engineering and Joint Program for Advanced Electronic Materials, University of Maryland Baltimore County, Baltimore, Maryland 21228*

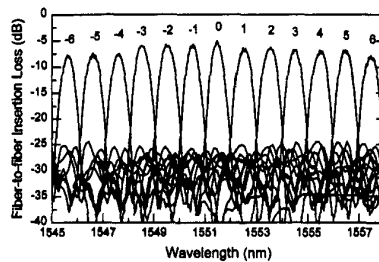
Phased-array waveguide grating (PAWG) device has become an important building block for optical wavelength-division multiplexing (WDM) communication systems. This is due, in part, to its low insertion loss, ease of fabrication, and integrability. Besides serving the basic function as a WDM multiplexer<sup>1</sup> or demultiplexer, it has also been applied to add/drop multiplexers,<sup>2</sup> frequency-selective switches and filters.<sup>3,4</sup> In this paper we present a novel 2 x N PAWG design, which utilizes two sets of vernier input ports to compensate center wavelength shifting due to processing.<sup>5</sup> By having two corresponding sets of output waveguides, each PAWG can function as two identical 1 x N-channel wavelength multi/demultiplexers. All input and output channels of the two 1 x N devices are interleaved to yield uniformity and efficient interconnect to cross-bar switches. An 8-channel wavelength-selective 2 x 2 nonblocking optical switch is designed using two 2 x 8 PAWGs, con-



**CFG1 Fig. 1** Schematic illustration of the 2 x N phased-array waveguide grating device.



**CFG1 Fig. 2** Schematic configuration of 8-channel wavelength-selective 2 x 2 switch base on two 2 x 8 PAWG devices.



**CFG1 Fig. 3** Fiber-to-fiber insertion loss spectrum of the silica waveguide-based PAWG device.

ected by 12 thermal-optic (TO) cross-bar switches. This 2 x 2 WDM optical switch can route each input wavelength to either output ports and is suitable for any transparent optical WDM network systems.

Figure 1 shows schematically the 2 x 8 PAWG design. On the O-port side, there are twelve pairs of waveguides, which are spaced by a constant angle  $2\alpha$ . The angle between the two waveguides in each pair is  $\alpha$ . Under this design, each of the two sets of waveguide channels has a constant wavelength spacing of  $\Delta\lambda = n_s d (2\alpha) / m$ , where  $d$  is the grating period of the PAWG,  $n_s$  is the effective index of the slab waveguide,  $m$  is the diffraction order, and  $2\alpha \ll 1$ . On the I-port side, there are five pairs of waveguides, which are spaced by a constant angle  $\beta$ . The angle between the two waveguides in each pair is  $\alpha$ . When the  $j$ -th channel pair at the I-port is used as the input ports, two sets of eight different demultiplexed wavelengths, with the same constant channel spacing  $\Delta\lambda$ , are output from  $(-3-j)$  to  $(4-j)$  and  $(-3'-j')$  to  $(4'-j')$  at O-port correspondingly. The output wavelength, at the  $j$ -th port is:  $\lambda_j(j) = n_s \Delta L / m + \Delta\lambda[(\beta/2\alpha) + j]$ . We noted that, if  $\beta \neq 2\alpha$ , the absolute wavelengths of output are different with different input port  $j$ . Using five input channels and  $\beta = 1.2 \times (2\alpha)$ , the absolute center channel wavelength can be adjusted to within  $\Delta\lambda/5$ .

Based on the above 2 x N multi/demultiplexer, we have designed an 8-channel wavelength-selective 2 x 2 optical switch, as shown in Fig. 2. The two

PAWGs are placed with overlapping slab waveguide regions. Both PAWGs have the same grating parameters described above, with a designed center wavelength of 1550 nm, a constant wavelength spacing  $\Delta\lambda = 1$  nm, and a free spectral range of 19.6 nm. Each chain pair at the O-port of the input PAWG is connected to the corresponding pair at the O-port of the output PAWG by a thermo-optical cross-bar switch.

The 2 x 2 optical switch is made monolithically by silica waveguide on silicon, using flame hydrolysis method. Figure 3 shows the insertion loss spectrum of the PAWG in the switch. The fiber-to-fiber loss is from -5 to -7.5 dB across the free spectral range. Because only the central portion of the free spectral range will be used, we expect the on chip loss of the device to be within 10 dB and a spectral response uniformity of ~3 dB. Detailed performance results are reported.

1. C. Dragone, *IEEE Photonics Technol. Lett.* 3, 812 (1991).
2. K. Okamoto, K. Takiguchi, Y. Ohmori, *Electron. Lett.* 31, 723 (1995).
3. O. Ishida, H. Takahashi, S. Suzuki, Y. Inoue, *IEEE Photon. Technol. Lett.* 6, 1219 (1994).
4. O. Ishida, H. Takahashi, Y. Inoue, *Electron. Lett.* 30, 1327 (1994).
5. H. Uetsuka, K. Akiba, H. Okano, Y. Kurosawa, K. Morosawa, in *Optical Fiber Communication Conference*, Vol. 8, 1995 OSA Technical Digest Series (Optical Society of America, Washington, DC, 1995), paper Tu07, p. 276.

**CFG2** 10:45 am

**Distributed feedback lasers integrated with micromachined wavelength meters for dense WDM systems**

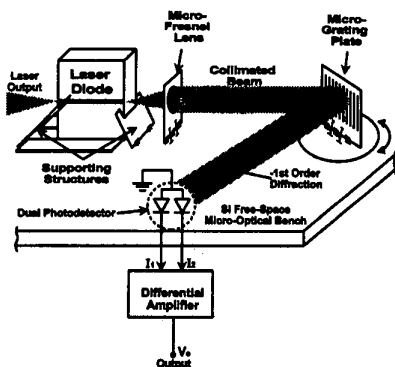
S. S. Lee, L. Y. Lin, M. C. Wu, *UCLA, Electrical Engineering Department, Room 66-147D Engineering IV, Box 951594, Los Angeles, California 90095-1594*

Single-wavelength semiconductor lasers with wavelength monitoring capability are very important for dense wavelength-division multiplexed (WDM) communication systems. Monolithic integration of distributed feedback (DFB) or distributed Bragg reflector (DBR) laser with waveguide-type spectrometer could be realized by photonic integrated circuit (PIC). However, the spectrometer occupies a very large area, which results in low yield and high cost. Furthermore, the wavelength matching between the lasers and the spectrometer further complicates the fabrication tolerance. On the other hand, very-low-cost free-space microspectrometers can be mass-produced by the surface-micromachining technique on Si substrate. By combining the DFB laser or the WDM laser array with the microspectrometer on the Si free-space micro-optical bench (FSMOB), low-cost and high-performance WDM source can be obtained. In this paper, we believe we re-

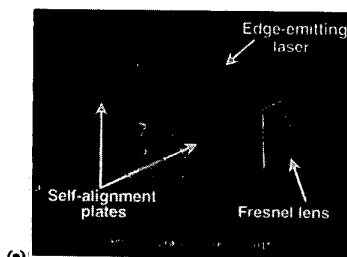


port on the first demonstration of the free-space micro-optical system consisting of a DFB laser and a surface-micromachined precision wavelength-meter on a Si micro-optical bench.

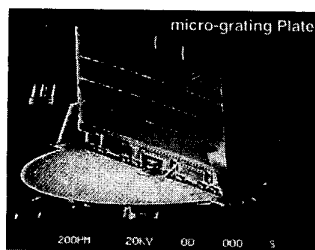
The schematic diagram of the free-space micro-optical system is shown in Fig. 1. The wavelength-meter consists of a collimating micro-Fresnel lens, a rotatable micro-grating,<sup>1</sup> and a dual-photodetector. The DFB laser is hybrid-mounted on the Si substrate using a self-aligned hybrid integration scheme.<sup>2</sup> All the micro-optical elements are batch fabricated and have been "pre-aligned" during the layout of the photomasks. The scanning



CFG2 Fig. 1 The schematic diagram of the DFB laser integrated with a precision wavelength meter on a free-space Si micro-optical bench.

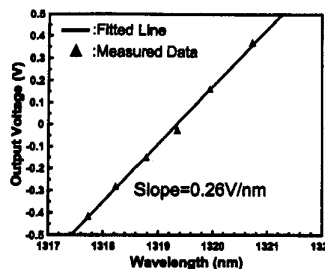


(a)



(b)

CFG2 Fig. 2 The SEM micrographs of (a) the self-aligned semiconductor laser mounted on free-space micro-optical bench, and (b) the surface-micromachined three-dimensional micro-grating.



CFG2 Fig. 3 The output voltage of the wavelength meter versus the laser wavelength.

electron micrographs (SEM) of the self-aligned semiconductor laser and the micro-grating are shown in Figs. 2(a) and 2(b), respectively. The reflective grating has a pitch of  $4 \mu\text{m}$  and an area of  $400 \mu\text{m} \times 950 \mu\text{m}$ . The wavelength meter is first calibrated by rotating the grating so that the first-order diffracted beam shines uniformly on the dual-photodetector. The photocurrents are fed to a differential amplifier with a gain of 1000. The output signal is proportional to the difference of the photocurrents, and is zero at the calibrated wavelength. The change of laser wavelength causes a change of diffraction angle, which results in a nonzero differential photocurrent. The output voltage versus laser wavelength is plotted in Fig. 3. From the plot, the sensitivity of the wavelength monitor is estimated to be  $0.26 \text{ V/nm}$ . The wavelength measurement range of  $3 \text{ nm}$  is limited by thermal tuning range of the DFB laser. The resolution is experimentally observed to be  $0.3 \text{ nm}$ . Resolution better than  $0.1 \text{ nm}$  is achievable by further optimization. The output from the wavelength meter can be used to stabilize the output wavelength or lock the output wavelength of the DFB laser to the specified wavelength. The rotatable grating allows the wavelength meter to be used for a wide range of wavelengths. The Ge dual photodetector can also be integrated on the same Si substrate to eliminate possible mechanical vibrations. The wavelength meter can be turned into a micro-spectrometer by replacing the dual photodetector with a photodetector array.

In conclusion, a single-chip micro-optical system consists of a DFB laser and a surface-micromachined precision wavelength meter on a Si free-space micro-optical bench has been demonstrated for the first time, to our knowledge. A wavelength sensitivity of  $0.26 \text{ V/nm}$ , and a resolution of  $0.3 \text{ nm}$  have been demonstrated. The photodetector and the electronic circuits could potentially be integrated on the same Si chip to realize a very compact, light weight and low-cost optical sources for dense WDM systems.

1. S. S. Lee, L. Y. Lin, M. C. Wu, Appl. Phys. Lett. 67, 2135–2137 (1995).
2. L. Y. Lin, S. S. Lee, K. S. J. Pister, M. C. Wu, Appl. Phys. Lett. 66, 2946–2948 (1995).

CFG3

11:00 am

### Low-loss eight-channel integrated InGaAsP/InP demultiplexer

G. H. B. Thompson, M. Asghari,\* S. J. Clements, S. M. Ojha, I. H. White,\* BNR Europe Limited, London Road, Harlow, Essex, CM17 9NA, U.K.

Integrated optical devices potentially offer significant advantages over their bulk counterparts in that they offer compactness, mass production (low unit cost), and relaxed alignment requirements. Fabrication in the InP material system provides the added advantage of active/passive device integration. A two-dimensional approach to integration is particularly suited to multiwavelength applications due to the effective parallelism required in such systems. In such an approach a grating structure can be incorporated within a slab structure to provide de/multiplexing of a large number of channels. Here the device loss is independent of the number of channels unlike in one-dimensional waveguide-based devices incorporating wavelength-dependent couplers,<sup>1,2</sup> where the device losses increase with the number of channels.

The successful operation of integrated self-focusing curved grating structures has been reported.<sup>3,4</sup> However, such devices are typically very large ( $>10 \text{ mm}$  in length) and exhibit high losses. Here an eight-channel demultiplexer device is reported, which incorporates a grating structure together with collimating and reflecting mirrors within the two-dimensional plane of a slab (Fig. 1). The diverging beam from the input waveguide propagates in the plane of the slab and illuminates a collimating reflector that directs the beams to the transmission grating. Dispersion by the grating causes the light to fall on an output focusing reflector and be directed to the corresponding output waveguide. The device, the smallest yet reported, measures  $2 \text{ mm} \times 1 \text{ mm}$  and is designed for a channel separation of  $4 \text{ nm}$ . The grating structure has a period of  $7.5 \mu\text{m}$  and operates in the 18th diffraction order at  $1.55\text{-}\mu\text{m}$  wavelength. Mirror structures have a focal length of  $1 \text{ mm}$  and the waveguides are  $2.5\text{-}\mu\text{m}$  wide and separated by  $10 \mu\text{m}$  at the output. The incidence angles on the mirror and grating elements are  $22.5^\circ$  and  $45^\circ$  respectively. In this case, as in the four-channel demultiplexer previously reported,<sup>5</sup> the use of mirror structures enables improved grating performance and allows operation above the critical angle for low reflection losses.

Figure 2 represents the loss distribution obtained from testing a large number of such structures. Total device losses as low as  $8 \text{ dB}$  have been measured with mirror losses typically in the range  $1$  to  $2 \text{ dB}$ . The major loss contribution has resulted from rounding of the grating element corners due to imperfect patterning at the lithographic stage of fabrication. A typical two-dimensional near-field plot of the demultiplexer is shown in Fig. 3. A full width half maximum (FWHM) value of  $2.7 \mu\text{m}$  is measured for the output op-